SODIUM NITRITE IMPACTS THE PERIPHERAL CONTROL OF CONTRACTING SKELETAL MUSCLE MICROVASCULAR OXYGEN PRESSURE IN HEALTHY RATS

by

TRENTON DAVID COLBURN

B.S., Kansas State University, 2016

A THESIS

submitted in partial fulfillment of the requirements for the degree

MASTER OF SCIENCE

Department of Kinesiology
College of Human Ecology

KANSAS STATE UNIVERSITY
Manhattan, Kansas

2016

Approved by:

Major Professor
Dr. Timothy I. Musch

Copyright

Abstract

Exercise intolerance characteristic of diseases such as chronic heart failure (CHF) and diabetes is associated with reduced nitric oxide (NO) bioavailability from nitric oxide synthase (NOS), resulting in an impaired microvascular O_2 driving pressure (PO_2mv: O_2 delivery – O_2 utilization) and metabolic control. Infusions of the potent NO donor sodium nitroprusside augment NO bioavailability yet decrease mean arterial pressure (MAP) thereby reducing its potential efficacy for patient populations. To eliminate or reduce hypotensive sequellae NO_2^- was superfused onto the spinotrapezius muscle. It was hypothesized that local NO_2^- administration would elevate resting PO_2mv and slow PO_2mv kinetics (increased τ: time constant, MRT: mean response time) following the onset of muscle contractions. In 12 anesthetized male Sprague-Dawley rats, PO_2mv of the circulation-intact spinotrapezius muscle was measured by phosphorescence quenching during 180 s of electrically-induced twitch contractions (1 Hz) before and after superfusion of $NaNO_2$ (30 mM). NO_2^- superfusion elevated resting PO_2mv (CON: 28.4 ± 1.1 vs NO_2^-: 31.6 ± 1.2 mmHg, $P \leq 0.05$), τ (CON: 12.3 ± 1.2 vs NO_2^-: 19.7 ± 2.2 s, $P \leq 0.05$) and MRT (CON: 19.3 ± 1.9 vs NO_2^-: 25.6 ± 3.3 s, $P \leq 0.05$). Importantly, these effects occurred in the absence of any reduction in MAP (103 ± 4 vs 105 ± 4 mmHg, pre- and post-superfusion respectively; $P > 0.05$). These results indicate that NO_2^- supplementation delivered to the muscle directly through NO_2^- superfusion enhances the blood-myocyte driving pressure of oxygen without compromising MAP at rest and following the onset of muscle contraction. This strategy has substantial clinical utility for a range of ischemic conditions.

Table of Contents

List of Figures

List of Tables

Acknowledgements

I would like to thank K. Sue Hageman for her superb technical assistance. Additionally, I am thankful for the incessant mentoring and support of Drs. Timothy I. Musch and David C. Poole as well as Drs. Clark T. Holdsworth and Scott K. Ferguson, and Jesse C. Craig.

Financial support for this research was provided by American Heart Association Midwest Affiliate (10GRNT4350011) and NIH (HL-108328) awards to David C. Poole.

Introduction

Sustained muscle contractions require a robust and appropriate hyperemic response that is contingent upon arteriolar vasodilation increasing muscle O_2 delivery ($\dot{Q}O_2$) in proportion to the elevated O_2 demands ($\dot{V}O_2$). It is also important to recognize that the instantaneous $\dot{Q}O_2$/ $\dot{V}O_2$ ratio sets microvascular O_2 pressures (PO_2mv) that are crucial for blood-myocyte O_2 flux and also the intracellular PO_2 which influences metabolic control (29, 50).

Within the spectrum of vasoactive mediators for the exercise hyperemia nitric oxide (NO) is a key player. Thus, blockade of the endogenous endothelial NO synthase (eNOS) and/or neuronal NOS (nNOS) systems reduces exercising muscles(s) blood flow and $\dot{Q}O_2$ (8, 28) lowering PO_2mv (22) and impairing function. In diseases such as chronic heart failure dysfunction of the NOS system reduces NO bioavailability with the resultant decrease of PO_2mv, especially in the transient phase immediately following the onset of contractions, slows $\dot{V}O_2$ kinetics and contributes to muscle dysfunction characteristic of chronic heart failure (CHF) (15, 21, 26, 44).

Given the reduced capacity for endogenous NO production in disease, possibly as a consequence of tissue hypoxia and elevated reactive oxygen species which constrain NOS function, there has been substantial interest in providing exogenous NO precursors such as sodium nitroprusside (SNP) and inorganic nitrate/nitrite (NO_3^-/NO_2^-) (37, 54). A particularly attractive feature of the NO_3^-/NO_2^- pathway is that the pathological muscle hypoxia found in CHF and other patients promotes NO_2^- reduction to NO and hence enhances $\dot{Q}O_2$ locally without compromising systemic blood pressure as might be expected for systemic vasodilators such as SNP or hydralazine, for example (51, 52). Recently, beetroot (BR) juice has been advocated as an NO_3^-/NO_2^- source that reduces mean arterial pressure, enhances muscle $\dot{Q}O_2$ and PO_2mv, and

improves muscle contractile function and efficiency (19, 20, 33). Unfortunately, after absorption in the gut the NO_3^--NO_2^- reduction requires salivary gland NO_3^- secretion and the participation of commensal bacteria in the oral cavity before resorption into the blood stream as circulating NO_2^-. These steps typically take hours to raise plasma [NO_2^-] (53) and can be blocked by mouthwash-induced bactericide (39).

Given these limitations the utility of increasing vascular [NO_2^-] more directly has been considered (38). However the results have been controversial with up to 36 μmol/min NO_2^- infused into the forearms of healthy subjects proving ineffective (34). Arguing that hypoxia is crucial for the NO_2^--NO reduction Maher and colleagues (38) subsequently demonstrated that direct arterial infusions into the resting forearm of subjects breathing 12% O_2 (estimated arterial PO_2 48-55 mmHg) induced a robust arterial vasodilation. These are precisely the conditions extant in the microvasculature of contracting muscles. Specifically, in the rat during exercise muscle PO_2mv falls to ~20 mmHg in muscles comprised predominantly of slow twitch fibers or ~10 mmHg in fast twitch muscles (4, 40). Moreover, we have demonstrated that, when NO bioavailability is reduced by CHF (23) or NOS blockade (18), NO_2^- infusions induce a robust increase in muscle $\dot{Q}O_2$ that is especially pronounced in fast twitch muscles.

Because enhanced NO bioavailability has the potential to both elevate $\dot{Q}O_2$ and reduce $\dot{V}O_2$ direct measurements of PO_2*mv* are necessary to evaluate the efficacy of NO_2^- treatment to enhance blood-myocyte O_2 flux. Moreover, because $\dot{V}O_2$ demands change most rapidly within the first minute or so of contractions we argue that assessing the efficacy of NO_2^- to raise PO_2mv across this interval with high temporal fidelity is crucial. In the rat spinotrapezius muscle we therefore tested the hypothesis that local NO_2^- superfusion under normoxic conditions would

elevate PO_2mv significantly and, importantly, would do so in the absence of systemic hypotension.

Methods

Twelve male Sprague-Dawley rats (mass = 421 ± 23 g, Charles River Laboratories, Wilmington, MA) were used in this investigation. Rats were provided food and water *ad libitum* while housed in a 12/12 hr light-dark cycle facility at Kansas State University. All procedures were approved by the Institutional Animal Care and Use Committee of Kansas State University and conducted according to National Institute of Health Guidelines.

Surgical Preparation

Rats were initially anesthetized with a 5% isoflurane-O_2 mixture and subsequently maintained on 3% isoflurane-O_2. Following cannulation of the carotid artery, a catheter (PE-10 connected to PE-50, Intra-Medic polyethylene tubing, Clay Adams Brand, Becton, Dickinson and Company, Sparks, MD) was inserted into the carotid artery for measurement of mean arterial pressure (MAP) and heart rate (HR), and infusion of the phosphorescent probe (see below). A second catheter was inserted into the caudal artery for the infusion of pentobarbital sodium anesthesia and arterial blood sampling. Upon closing the incisions for the carotid and caudal catheters, rats were transitioned to pentobarbital sodium anesthesia and concentrations of isoflurane were removed. The level of anesthesia was regularly monitored via toe pinch and palpebral reflex; with anesthesia supplemented as necessary. Rats were placed on a heating pad to maintain a core temperature of ~38˚C (measured via rectal probe). Incisions were then made to carefully expose the right spinotrapezius muscle with overlying skin and fascia reflected such that the integrity of the neural and vascular supply was maintained (2). Using 6-0 silk sutures, silver wire electrodes were secured to the rostral (cathode) and caudal (anode) regions of the muscle. Exposed muscle tissue was superfused with warmed (38 ˚C) Krebs-Henseleit

bicarbonate buffered solution equilibrated with 5% CO_2-95% N_2. Surrounding exposed tissue was covered with Saran wrap (Dow Brands, Indianapolis, IN) to ensure that superfused solutions were confined to the spinotrapezius. The spinotrapezius muscle was selected based on its mixed muscle fiber-type composition and citrate synthase activity, which resembles the quadriceps muscle in humans (13, 35).

Experimental Protocol

The phosphorescent probe palladium meso-tetra (4 carboxyphenyl)tetrabenzoporphyrin dendrimer (G2: 15-20 mg kg^{-1} dissolved in 0.4 ml saline) was infused via the carotid artery catheter. Following a brief stabilization period (~10 min), the common end of the light guide of a frequency domain phosphorimeter (PMOD 5000, Oxygen Enterprises, Philadelphia, PA) was positioned ~2-4 mm superficial to the dorsal surface of the exposed right spinotrapezius muscle as described previously (2). Fields containing large vessels were avoided in order to ensure that the measurements obtained were of principally capillary blood. PO_2mv was measured at rest and during the 180 s contraction protocol (1 Hz, ~6V, 2 ms pulse duration) via phosphorescence quenching (see below) and recorded at 2 s intervals. Muscle contractions were elicited via a Grass stimulator (model S88, Quincy, MA). Following the contraction period, blood samples were taken for analysis and PO_2mv was monitored to ensure that microvascular control was preserved and values returned to baseline. After a 30 min stabilization period $NaNO_2$ (30 mM in 3.0 ml Krebs-Henseleit bicarbonate buffered solution) was continuously superfused for 3 min along the exposed muscle. This $NaNO_2$ dose was chosen due to the curved nature of the spinotrapezius muscle spanning the rib cage. Once the superfused solution is applied, the portion that does not diffuse into the muscle runs down the Saran wrap and onto a waste collection site.

Approximately 1 min following superfusion, after PO_2mv stabilized, the aforementioned contraction protocol was repeated. Rats were then euthanized via pentobarbital sodium overdose (≥50 mg/kg administered into the carotid artery catheter).

PO_2mv Measurement and Curve-fitting

PO_2mv was calculated using the Stern-Volmer relationship. Direct measurement of phosphorescence lifetime utilized in the following equation yields PO_2mv (45);

$$PO_2mv = [\ \tau^\circ / \tau - 1] / (k_Q \ x \ \tau^\circ)$$

Where k_Q is the quenching constant and τ° and τ are the phosphorescence lifetimes in the absence of O_2 and at the ambient O_2 concentration, respectively. For G2, k_Q is 273 $mmHg^{-1}\ s^{-1}$ and τ° is 251 μs (16). Since the G2 phosphorescent probe binds to blood proteins, G2 is evenly distributed throughout plasma and compartmentalized to the vascular space (16, 43). Therefore, *in vivo*, the phosphorescence lifetimes are determined directly by O_2 pressure because k_Q and τ° do not change appreciably over the physiological ranges of temperature and pH (16, 45).

Using computer software (SigmaPlot 11.0, Systat Software, San Jose, CA), PO_2mv responses were curve-fitted from the collected PO_2mv data points. Curves were fit using either one-component or two-component models described below:

One component: $PO_2mv_{(t)} = PO_2mv_{(BL)} - \Delta\ PO_2mv\ (1- e^{-(t - TD)/t})$

Two component: $PO_2mv_{(t)} = PO_2mv_{(BL)} - \Delta_1 PO_2mv\ (1- e^{-(t - TD_1)/\tau_1}) + \Delta_2 PO_2mv\ (1- e^{-(t - TD_2)/\tau_2})$

Where $PO_2mv_{(t)}$ represents the PO_2mv at any given time t, PO_2mv_{BL} corresponds to the pre-contracting resting baseline PO_2mv, Δ_1 and Δ_2 are the amplitudes for the first and second component, respectively, TD_1 and TD_2 are the time delays for each component, and τ_1 and τ_2 are

the time constants (i.e., time to reach 63% of the final response value) for each component. Appropriate fits were determined using the following criteria: 1) the coefficient of determination, 2) sum of the squared residuals, 3) visual inspection and analysis of the model fits to the data and the residuals. To provide an index of the overall principal kinetics response, the first and second components were used to calculate MRT_1 and MRT_2, respectively. MRT was calculated using the following equations:

One component: $MRT_1 = TD_1 + \tau_1$

Two component: $MRT_2 = TD_2 + \tau_2$

Where TD_1, TD2, τ_2 and τ_2 are as described above.

Statistical Analysis

Data are presented as means ± SE. Preliminary data were compared between (Superfusion vs. IA Infusion) and within groups using two-way repeated measures ANOVA (MAP) with Tukey's post hoc analyses. Study results were compared within (Pre- vs. Post-Superfusion) groups using one-way repeated measures ANOVA (MAP and HR) or paired 1- and 2- tail Student's t-tests as appropriate for a priori directional hypotheses (blood gases, blood [lactate], and PO_2*mv* kinetics parameters). Significance was accepted at $P \leq 0.05$.

Results

Preliminary data (n=3) in Figures 1 and 2 indicated that $NaNO_2$ (30 mM) during a 3-min superfusion protocol elevated PO_2mv without significantly changing MAP. Bolus intra-arterial (IA) infusion (7 mg kg^{-1}) decreased MAP significantly and transiently decreased PO_2mv within the initial 3-min.

Microvascular Oxygen Pressures (PO_2mv)

Within 3-min superfusion of $NaNO_2$ PO_2mv was significantly elevated (PO_2mv_{BL}; CON: 28.4 ± 1.1 mmHg vs. NO_2^-: 31.6 ± 1.2; $P \leq 0.05$) (Table 1, Figure 3). Following the onset of contractions, NO_2^- exhibited a significantly larger PO_2mv amplitude (CON: 10.5 ± 0.9 vs. NO_2^-: 12.7 ± 0.8 mmHg; $P \leq 0.05$), slower τ (CON: 12.3 ± 1.2 vs. NO_2^-: 19.7 ± 2.2 s; $P \leq 0.05$), and increased MRT (CON: 19.3 ± 1.9 vs. NO_2^-: 25.6 ± 3.3 s; $P \leq 0.05$) (Figure 4A). As shown in Figure 4B, the difference in driving pressure between conditions continued for the first 40 seconds of electrically-stimulated contractions.

Central Hemodynamics and Blood Gases

Superfusion of $NaNO_2$ did not significantly alter MAP or HR from pre-superfusion values (MAP: 103 ± 4 vs. 105 ± 4 mmHg, HR: 330 ± 10 vs. 321 ± 11 bpm, pre- and post- respectively; both $P > 0.05$). Likewise, there was no significant difference in MAP or HR between CON and NO_2^- conditions following the contraction protocol ($P > 0.05$). Finally, there were no significant differences in $\%O_2$ saturation (CON: 91.5 ± 1.5 vs. NO_2^-: 93.1 ± 0.7%), PCO_2 (CON: 42 ± 2 vs. NO_2^-: 41 ± 2 mmHg), or blood [lactate] (CON: 1.6 ± 0.1 vs. NO_2^-: 1.6 ± 0.2 mM) between groups ($P > 0.05$).

Table 1. PO_2mv parameters of the spinotrapezius muscle at rest and following the onset of contractions under control and $NaNO_2$ conditions

	CON	NO_2^-
PO_2mv_{BL}, mmHg	28.4 ± 1.1	31.6 ± 1.2*
Δ_1PO_2mv, mmHg	10.5 ± 0.9	12.7 ± 0.8*
$PO_2mv_{(steady\text{-}state)}$, mmHg	18.0 ± 0.9	18.9 ± 1.2
TD_1, s	7.0 ± 1.2	6.0 ± 1.6
τ_1, s	12.3 ± 1.2	19.7 ± 2.2*
MRT_1, s	19.3 ± 1.9	25.6 ± 3.3*
Δ_2PO_2mv, mmHg	3.4 ± 0.5	2.9 ± 0.1
TD_2, s	78.5 ± 22.3	68.9 ± 9.5
τ_2, s	67.9 ± 7.7	77.1 ± 14.2
MRT_2, s	146.4 ± 25.7	97.3 ± 48.8

Values are means ± SE. PO_2mv_{BL}, resting PO_2mv; Δ_1PO_2mv and Δ_2PO_2mv amplitude of the first and second components; $PO_2mv_{(steady\text{-}state)}$, contracting steady-state PO_2mv; TD_1 and TD_2, time delay of the first and second component; τ_1, and τ_2, time constant of the first and second component; MRT_1 and MRT_2, mean response time of the first and second component. Primary components were calculated for all rats (n=12). Secondary components were present in 3 CON and 2 NO_2^- rats. *$P \leq 0.05$ vs. CON.

Figure 1. $NaNO_2$ Superfusion vs. Intra-arterial Infusion on PO_2mv

Averaged PO_2mv from preliminary results (n=3) during 180 s of $NaNO_2$ superfusion (30 mM) and a bolus intra-arterial (IA) infusion of $NaNO_2$ (7 mg kg^{-1}). Inset black box denotes the superfusion period. Measurements were recorded for an additional 600 s to monitor the effects of direct vs. systemic administration in the absence of muscle contraction. Following a plateau in PO_2mv, there was a decline in PO_2mv at the rate of -0.012 mmHg s^{-1} in the superfusion condition.

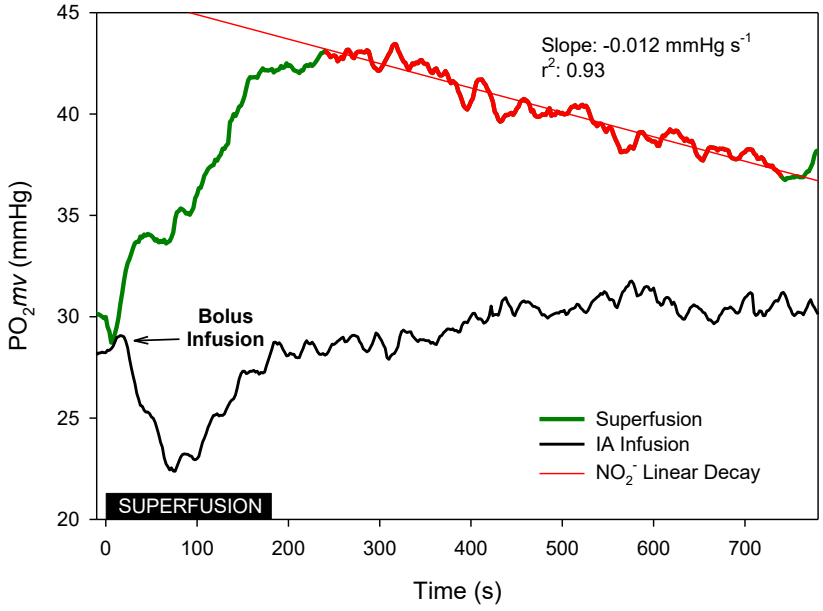

Figure 2. $NaNO_2$ Superfusion vs. Intra-arterial Infusion on MAP

Preliminary results (n=3) showed that mean arterial pressure (MAP) during 180 s of $NaNO_2$ superfusion (30 mM) remained constant whereas a bolus intra-arterial (IA) infusion of $NaNO_2$ (7 mg kg^{-1}) produced a sustained reduction in MAP by as much as ~14-15 mmHg. Data are presented as means ± SE.

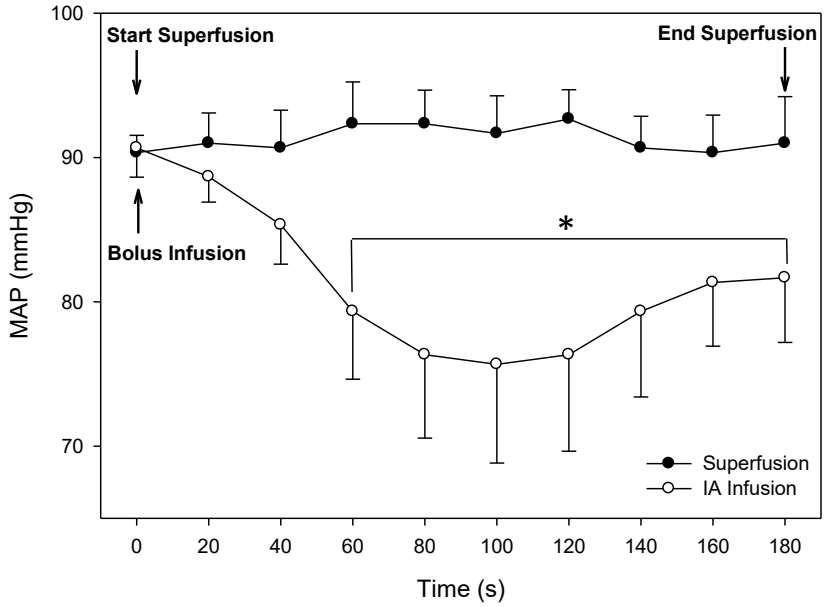

Figure 3. Microvascular oxygen pressure (PO_2mv) during $NaNO_2$ superfusion

Microvascular oxygen pressure (PO_2mv) of the spinotrapezius muscle for the experimental group of rats (n=12) was measured every 2 s during the 180 s superfusion of 30 mM $NaNO_2$ in Krebs-Henseleit solution. Inset black box denotes the superfusion period.

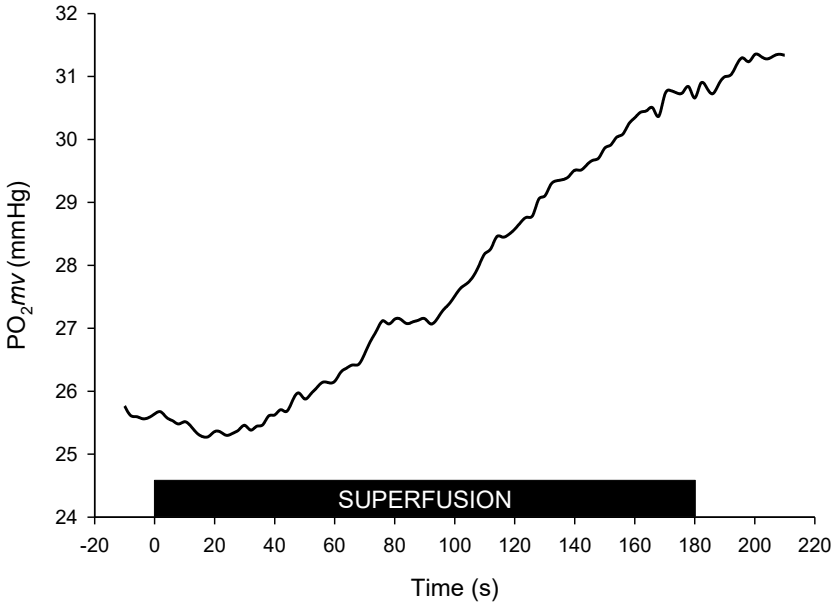

Figure 4. PO_2mv and MAP during contractions, and PO_2mv difference between $NaNO_2$ and Control

A: Average spinotrapezius PO_2mv kinetics for the experimental group of rats (n=12) during 180 s electrically stimulated contractions in the control condition (closed circles) and following $NaNO_2$ superfusion (open circles). Mean arterial pressure (closed squares) was recorded at the beginning and end of the contraction protocol. Data are presented as means ± SE. B: PO_2mv differences for each 2 s measurement for the experimental group of rats (n=12) between $NaNO_2$ and CON conditions during spinotrapezius muscle contractions. Note that prior to (i.e. left of) the dashed line, $NaNO_2$ is significantly different from CON ($P < 0.05$).

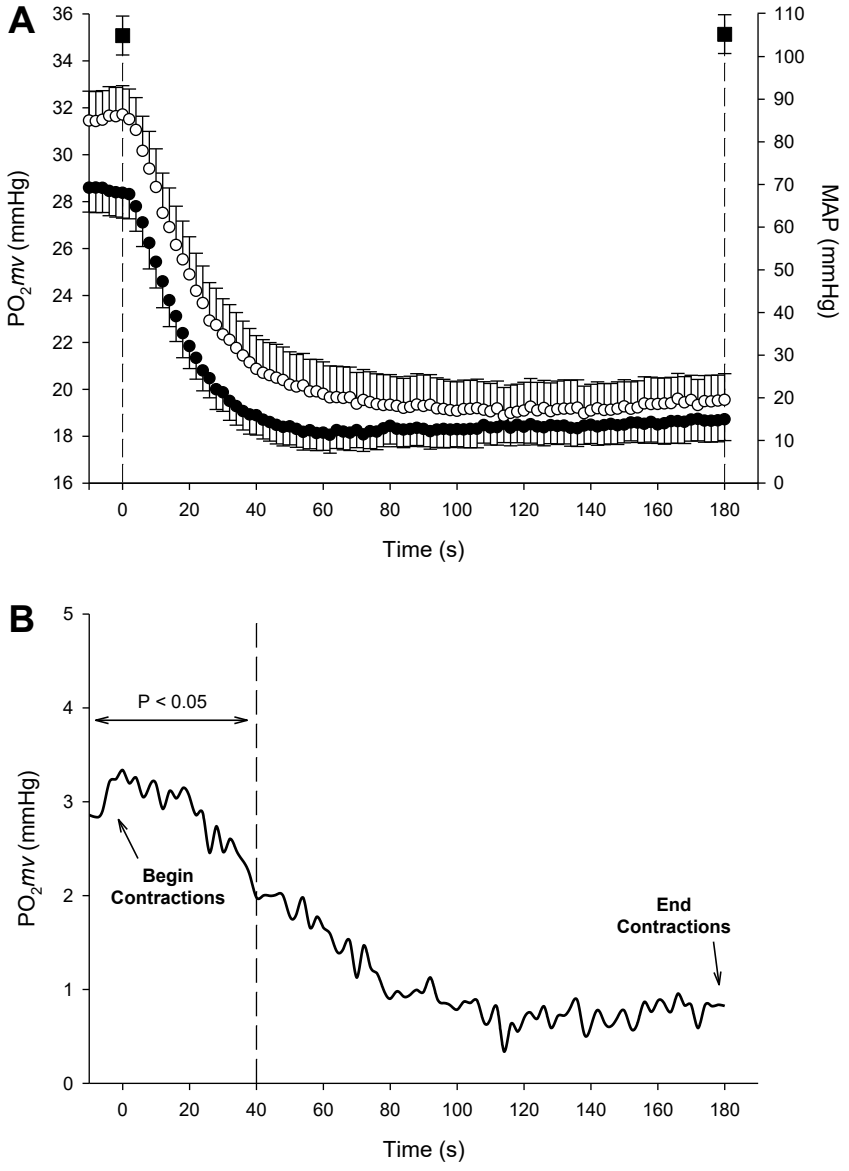

Discussion

The principal original findings of the present investigation demonstrate that $NaNO_2$ superfusion enhances the muscle PO_2mv at rest (i.e. elevated PO_2mv_{BL}) and during the transition from rest-to-contractions, in part, by slowing the PO_2mv fall (i.e. increased τ and MRT). Importantly, these effects occurred concomitant with stable MAP. The ability of NO_2^- to enhance the driving pressure of O_2 before and for the 40 s after the onset of muscle contractions (Figures 4A and 4B) would be expected to potentially decrease reliance on immediate, nonoxidative energy pathways and delay the production of fatigue-inducing metabolic products (29, 50). In disease conditions attended by cardiovascular complications, the inability to deliver O_2 may induce ischemic damage, impair recovery and, for active skeletal muscle, constrain exercise performance and perhaps daily activities essential to life quality. The delivery of exogenous NO_2^- is known to improve the central and systemic derangements prevalent in CHF (5, 37, 42) and we now demonstrate that it rapidly enhances peripheral control directly by circumventing the NOS pathway.

Microvascular Oxygen Pressure (PO_2mv) Dynamics

In skeletal muscle at rest, $NaNO_2$ has the potential to elevate the driving pressure of O_2 from blood to myocyte (PO_2mv_{BL}) under normoxic conditions. This NOS-independent effect coheres with previous investigations that have administered NO precursors (20, 22, 25). With respect to the PO_2mv elevations, these may be the consequence of increased $\dot{Q}O_2$, decreased $\dot{V}O_2$, or a combination of both. $\dot{Q}O_2$ increases with increasing $[NO_2^-]$ because the one step reduction to NO occurs in the low PO_2 environment of resistance vessels in healthy individuals (18, 19). The advantage of the NO_2^--NO reduction is that NOS reliance is avoided, rather NO_2^- is

reduced to NO in environments of low O_2/pH via interactions with deoxyhemoglobin, tissue and vascular myoglobin, xanthine oxidoreductase, and aldehyde dehydrogenase. Furthermore, by experimental blockade of endogenous production of NO from eNOS and nNOS pharmacologically (L-NAME and SMTC) blood flow is reduced independent of any increases in sympathetic activity/vasoconstriction (10, 27)(9, 10, 27, 28). The present results clearly demonstrate that $NaNO_2$ increases PO_2mv_{BL} and that the NO_2^--NO reduction compliments any NO emanating from the intact NOS system to augment PO_2mv. The direct measurement of PO_2mv herein extends previous observations of NO_2^- induced vasorelaxation and increased $\dot{Q}O_2$ in healthy subjects (11, 12, 38).

Potentially, the increased PO_2mv could also be explained by mitochondrial inhibition ($\downarrow\dot{V}O_2$) where NO competitively binds to complexes I and IV of the respiratory chain (6, 7). However, if the primary effect of NO_2^- on PO_2mv is mitochondrial inhibition, then a continuous increase in steady-state PO_2mv during muscle contractions would be expected but clearly this is not found (Figure 4A). It is pertinent that using a similar protocol with SNP, Hirai and colleagues (25) demonstrated the integrity of mitochondrial respiration (and thus $\dot{V}O_2$) concomitant with elevated NO_2^- and NO. Thus, the elevation in baseline PO_2mv seen herein is most likely the consequence of enhanced blood flow and $\dot{Q}O_2$ rather than decreased $\dot{V}O_2$.

The heightened vascular response and increased QO_2 with $NaNO_2$ superfusion (11, 28, 46) persists into the onset of contractions (slowed PO_2mv kinetics) as demonstrated in Figures 4A and 4B. In Figure 4B the rate at which PO_2mv is falling is slowed by disproportionate changes in $\dot{Q}O_2$ and $\dot{V}O_2$ across the initial 40 seconds. Enhancing the $\dot{Q}O_2$-to-$\dot{V}O_2$ relationship at this crucial transition would potentially improve energy production via oxidative metabolism,

decrease the acidic sequelae of glycolytic pathways, and delay the onset of fatigue processes (29, 50).

Potential Therapeutic Significance

NO_2^- precursors such as NO_3^- containing beetroot juice effectively increase plasma [NO_2^-] and can improve exercise performance in healthy individuals (1, 32, 53) and patient populations where cardiovascular function is impaired such as CHF (54) and peripheral artery disease (PAD) (31). Specifically, CHF patients have an increased cardiac output reserve secondary to the reduction of vascular resistance (54). Likewise, PAD patients exhibit improved exercise/walking performance and delayed onset of claudication following beetroot juice supplementation (31). However, elevating circulating [NO_2^-] via dietary means takes 2-3 hours which may constitute too great a delay for an effective therapeutic outcome. A potential alternative is oral administration of $NaNO_2$ which elevates circulating [NO_2^-] within 30 minutes in older adults (14) and diabetic patients (24). More direct routes of $NaNO_2$ (i.e. intravascular infusion or oral administration) can bypass the need for bacterial breakdown of NO_3^- and absorption in the gut and increase vascular [NO_2^-] rapidly. Thus, i.v. NO_2^- infusions have improved cardiac function and exercise performance in CHF patients (5). Additionally, NO_2^- infusion during L-NAME induced NOS blockade or CHF (18, 23) reverses the consequences of absent endogenous NO bioavailability and provides an avenue for enhanced $\dot{Q}O_2$-to-$\dot{V}O_2$ matching.

Administration of $NaNO_2$ protects against hypoxic damage to liver, cerebral, and myocardial tissue via the reduction of NO_2^- to NO (17, 30, 47, 49), but possibly not the kidney (3, 48). Therefore topical administration of $NaNO_2$, potentially via implantable osmotic micro-pump, may provide tissue protection during acute surgical or other medical conditions by

elevating $\dot{Q}O_2$ and PO_2mv within 3 minutes of application (see Figure 3) without confounding peripheral vascular effects (i.e. reductions in tissue PO_2mv [Figure 1] that are coincident with reductions in MAP [Figure 2]). Local administration may open up the avenue for long-term administration at a desired location enhancing $\dot{Q}O_2$ and PO_2mv for extended durations. The progressive decay of NO_2^-'s effects on PO_2mv (Figures 1 and 4B) indicates that setting the required [$NaNO_2$] and timing of application would be crucial.

Experimental Considerations

Although PO_2mv was significantly different at rest and the beginning of muscle contractions, the effect of NO_2^- is largely diminished by the time the steady-state PO_2mv is reached (Figure 4A and 4B). It remains unclear whether this is a direct effect of NO_2^- wearing off irrespective of muscle contractions, or whether contractions and the attendant hypoxia are elevating NO_2^- utilization. Figure 1 demonstrates that in the absence of muscle contractions, PO_2mv plateaus and then declines at a rate of ~0.7 mmHg min^{-1} after superfusion has ceased. This would indicate, in part, why $NaNO_2$ superfusion does not enhance steady-state PO_2mv relative to the control condition. Importantly, the linear decay in PO_2mv sheds light on the utilization of NO_2^- in the absence of systemic circulation which continually delivers NO_2^- stores. Future investigations into various delivery methods of $NaNO_2$ (i.e. injectable pellets or cutaneous patches) may be warranted considering that the administration of NO_2^- augments PO_2mv at rest and during the rest-exercise transition.

Conclusion

$NaNO_2$ serves therapeutically as a hypoxic vasodilator with efficacy for improving exercise performance in patients with cardiovascular disease (1, 5, 36, 41, 42). The present

investigation demonstrates the ability of $NaNO_2$ to locally elevate skeletal muscle PO_2mv at rest and following the onset of contractions in the healthy rat without altering MAP. Enhancing the muscle vascular O_2 driving pressure via $NaNO_2$ would provide a fast-acting modality to potentially improve metabolic control and thus delay fatigue and/or hypoxic damage. Improving PO_2mv dynamics alongside what remains of the endogenous NOS system under these conditions, $NaNO_2$ may ameliorate perturbations in the $\dot{Q}O_2$-to-$\dot{V}O_2$ ratio commonly found in disease states such as CHF and PAD. Fast-acting improvements in both resting and exercise PO_2mv dynamics may add to the current standard of care in populations with limited exercise tolerance along with individuals that may be suffering from focal tissue hypoxia and/or ischemia (i.e. frostbite, PAD, stroke).

References

1. **Bailey JC**, **Feelisch M**, **Horowitz JD**, **Frenneaux MP**, **Madhani M**. Pharmacology and therapeutic role of inorganic nitrite and nitrate in vasodilatation. *Pharmacol Ther* 144: 303–20, 2014.

2. **Bailey JK**, **Kindig CA**, **Behnke BJ**, **Musch TI**, **Schmid-Schoenbein GW**, **Poole DC**. Spinotrapezius muscle microcirculatory function: effects of surgical exteriorization. *Am J Physiol Hear Circ Physiol* 279: H3131–3137, 2000.

3. **Basireddy M**, **Isbell TS**, **Teng X**, **Patel RP**, **Agarwal A**. Effects of sodium nitrite on ischemia-reperfusion injury in the rat kidney. *Am J Physiol Renal Physiol* 290: F779–86, 2006.

4. **Behnke BJ**, **McDonough P**, **Padilla DJ**, **Musch TI**, **Poole DC**. Oxygen exchange profile in rat muscles of contrasting fibre types. *J Physiol* 549: 597–605, 2003.

5. **Borlaug BA**, **Koepp KE**, **Melenovsky V**. Sodium Nitrite Improves Exercise Hemodynamics and Ventricular Performance in Heart Failure With Preserved Ejection Fraction. *J Am Coll Cardiol* 66: 1672–1682, 2015.

6. **Brown GC**. Nitric oxide as a competitive inhibitor of oxygen consumption in the mitochondrial respiratory chain. *Acta Physiol Scand* 168: 667–74, 2000.

7. **Clementi E**, **Brown GC**, **Feelisch M**, **Moncada S**. Persistent inhibition of cell respiration by nitric oxide: Crucial role of S-nitrosylation of mitochondrial complex I and protective action of glutathione. *Proc Natl Acad Sci* 95: 7631–7636, 1998.

8. **Copp SW**, **Hirai DM**, **Ferguson SK**, **Holdsworth CT**, **Musch TI**, **Poole DC**. Effects of chronic heart failure on neuronal nitric oxide synthase-mediated control of microvascular O2 pressure in contracting rat skeletal muscle. *J Physiol* 590: 3585–96, 2012.

9. **Copp SW**, **Hirai DM**, **Schwagerl PJ**, **Musch TI**, **Poole DC**. Effects of neuronal nitric oxide synthase inhibition on resting and exercising hindlimb muscle blood flow in the rat. *J Physiol* 588: 1321–31, 2010.

10. **Copp SW**, **Hirai DM**, **Sims GE**, **Fels RJ**, **Musch TI**, **Poole DC**, **Kenney MJ**. Neuronal nitric oxide synthase inhibition and regional sympathetic nerve discharge: implications for peripheral vascular control. *Respir Physiol Neurobiol* 186: 285–9, 2013.

11. **Cosby K**, **Partovi KS**, **Crawford JH**, **Patel RP**, **Reiter CD**, **Martyr S**, **Yang BK**, **Waclawiw MA**, **Zalos G**, **Xu X**, **Huang KT**, **Shields H**, **Kim-Shapiro DB**, **Schechter AN**, **Cannon RO**, **Gladwin MT**. Nitrite reduction to nitric oxide by deoxyhemoglobin vasodilates the human circulation. *Nat Med* 9: 1498–505, 2003.

12. **Dejam A**, **Hunter CJ**, **Tremonti C**, **Pluta RM**, **Hon YY**, **Grimes G**, **Partovi K**, **Pelletier MM**, **Oldfield EH**, **Cannon RO**, **Schechter AN**, **Gladwin MT**. Nitrite infusion in humans and nonhuman primates: endocrine effects, pharmacokinetics, and tolerance formation. *Circulation* 116: 1821–31, 2007.

13. **Delp MD**, **Duan C**. Composition and size of type I, IIA, IID/X, and IIB fibers and citrate synthase activity of rat muscle. *J Appl Physiol* 80: 261–270, 1996.

14. **DeVan AE**, **Johnson LC**, **Brooks FA**, **Evans TD**, **Justice JN**, **Cruickshank-Quinn C**, **Reisdorph N**, **Bryan NS**, **McQueen MB**, **Santos-Parker JR**, **Chonchol MB**, **Bassett CJ**, **Sindler AL**, **Giordano T**, **Seals DR**. Effects of sodium nitrite supplementation on vascular function and related small metabolite signatures in middle-aged and older adults. *J Appl Physiol* 120: 416-425, 2016.

15. **Diederich E**. Dynamics of microvascular oxygen partial pressure in contracting skeletal muscle of rats with chronic heart failure. *Cardiovasc Res* 56: 479–486, 2002.

16. **Dunphy I**, **Vinogradov SA**, **Wilson DF**. Oxyphor R2 and G2: phosphors for measuring oxygen by oxygen-dependent quenching of phosphorescence. *Anal Biochem* 310: 191–198, 2002.

17. **Duranski MR**, **Greer JJM**, **Dejam A**, **Jaganmohan S**, **Hogg N**, **Langston W**, **Patel RP**, **Yet S-F**, **Wang X**, **Kevil CG**, **Gladwin MT**, **Lefer DJ**. Cytoprotective effects of nitrite during in vivo ischemia-reperfusion of the heart and liver. *J Clin Invest* 115: 1232–40, 2005.

18. **Ferguson SK**, **Glean AA**, **Holdsworth CT**, **Wright JL**, **Fees AJ**, **Colburn TD**, **Stabler T**, **Allen JD**, **Jones AM**, **Musch TI**, **Poole DC**. Skeletal Muscle Vascular Control During Exercise: Impact of Nitrite Infusion During Nitric Oxide Synthase Inhibition in Healthy Rats. *J. Cardiovasc. Pharmacol. Ther* 21: 201-208, 2016.

19. **Ferguson SK**, **Hirai DM**, **Copp SW**, **Holdsworth CT**, **Allen JD**, **Jones AM**, **Musch TI**, **Poole DC**. Impact of dietary nitrate supplementation via beetroot juice on exercising muscle vascular control in rats. *J Physiol* 591: 547–57, 2013.

20. **Ferguson SK**, **Hirai DM**, **Copp SW**, **Holdsworth CT**, **Allen JD**, **Jones AM**, **Musch TI**, **Poole DC**. Effects of nitrate supplementation via beetroot juice on contracting rat skeletal muscle microvascular oxygen pressure dynamics. *Respir Physiol Neurobiol* 187: 250–5, 2013.

21. **Ferreira LF**, **Hageman KS**, **Hahn SA**, **Williams J**, **Padilla DJ**, **Poole DC**, **Musch TI**. Muscle microvascular oxygenation in chronic heart failure: role of nitric oxide availability. *Acta Physiol (Oxf)* 188: 3–13, 2006.

22. **Ferreira LF**, **Padilla DJ**, **Williams J**, **Hageman KS**, **Musch TI**, **Poole DC**. Effects of altered nitric oxide availability on rat muscle microvascular oxygenation during contractions. *Acta Physiol* 186: 223–232, 2006.

23. **Glean AA**, **Ferguson SK**, **Holdsworth CT**, **Colburn TD**, **Wright JL**, **Fees AJ**, **Hageman KS**, **Poole DC**, **Musch TI**. Effects of nitrite infusion on skeletal muscle vascular control during exercise in rats with chronic heart failure. *Am J Physiol Heart Circ Physiol* 309: H1354-H1360, 2015.

24. **Greenway FL**, **Predmore BL**, **Flanagan DR**, **Giordano T**, **Qiu Y**, **Brandon A**, **Lefer DJ**, **Patel RP**, **Kevil CG**, **Ph D**. Single-dose pharmacokinetics of different oral sodium nitrite formulations in diabetes patients. *Diabetes Technol Ther* 14: 552–60, 2012.

25. **Hirai DM**, **Copp SW**, **Ferguson SK**, **Holdsworth CT**, **Musch TI**, **Poole DC**. The NO donor sodium nitroprusside: evaluation of skeletal muscle vascular and metabolic dysfunction. *Microvasc Res* 85: 104–11, 2013.

26. **Hirai DM**, **Musch TI**, **Poole DC**. Exercise training in chronic heart failure: improving skeletal muscle O2 transport and utilization. *Am J Physiol Heart Circ Physiol* 309: H1419–39, 2015.

27. **Hirai T**, **Musch TI**, **Morgan DA**, **Kregel KC**, **Claassen DE**, **Pickar JG**, **Lewis SJ**, **Kenney MJ**. Differential sympathetic nerve responses to nitric oxide synthase inhibition in anesthetized rats. *Am J Physiol* 269: R807–13, 1995.

28. **Hirai T**, **Visneski MD**, **Kearns KJ**, **Zelis R**, **Musch TI**. Effects of NO synthase inhibition on the muscular blood flow response to treadmill exercise in rats. *J Appl Physiol* 77: 1288–93, 1994.

29. **Hogan MC**, **Arthur PG**, **Bebout DE**, **Hochachka PW**, **Wagner PD**. Role of O2 in regulating tissue respiration in dog muscle working in situ. *J Appl Physiol* 73: 728–36, 1992.

30. **Jung K-H**, **Chu K**, **Ko S-Y**, **Lee S-T**, **Sinn D-I**, **Park D-K**, **Kim J-M**, **Song E-C**, **Kim M**, **Roh J-K**. Early intravenous infusion of sodium nitrite protects brain against in vivo ischemia-reperfusion injury. *Stroke* 37: 2744–50, 2006.

31. **Kenjale AA**, **Ham KL**, **Stabler T**, **Robbins JL**, **Johnson JL**, **Vanbruggen M**, **Privette G**, **Yim E**, **Kraus WE**, **Allen JD**. Dietary nitrate supplementation enhances exercise performance in peripheral arterial disease. *J Appl Physiol* 110: 1582–91, 2011.

32. **Larsen FJ**, **Schiffer TA**, **Borniquel S**, **Sahlin K**, **Ekblom B**, **Lundberg JO**, **Weitzberg E**. Dietary inorganic nitrate improves mitochondrial efficiency in humans. *Cell Metab* 13: 149–59, 2011.

33. **Larsen FJ**, **Weitzberg E**, **Lundberg JO**, **Ekblom B**. Effects of dietary nitrate on oxygen cost during exercise. *Acta Physiol (Oxf)* 191: 59–66, 2007.

34. **Lauer T**, **Preik M**, **Rassaf T**, **Strauer BE**, **Deussen A**, **Feelisch M**, **Kelm M**. Plasma nitrite rather than nitrate reflects regional endothelial nitric oxide synthase activity but lacks intrinsic vasodilator action. *Proc Natl Acad Sci U S A* 98: 12814–9, 2001.

35. **Leek BT**, **Mudaliar SRD**, **Henry R**, **Mathieu-Costello O**, **Richardson RS**. Effect of acute exercise on citrate synthase activity in untrained and trained human skeletal muscle. *Am J Physiol Regul Integr Comp Physiol* 280: R441–447, 2001.

36. **Lundberg JO**, **Weitzberg E**, **Gladwin MT**. The nitrate-nitrite-nitric oxide pathway in physiology and therapeutics. *Nat Rev Drug Discov* 7: 156–67, 2008.

37. **Maher AR**, **Arif S**, **Madhani M**, **Abozguia K**, **Ahmed I**, **Fernandez BO**, **Feelisch M**, **O'Sullivan AG**, **Christopoulos A**, **Sverdlov AL**, **Ngo D**, **Dautov R**, **James PE**, **Horowitz JD**, **Frenneaux MP**. Impact of chronic congestive heart failure on pharmacokinetics and vasomotor effects of infused nitrite. *Br J Pharmacol* 169: 659–70, 2013.

38. **Maher AR**, **Milsom AB**, **Gunaruwan P**, **Abozguia K**, **Ahmed I**, **Weaver RA**, **Thomas P**, **Ashrafian H**, **Born GVR**, **James PE**, **Frenneaux MP**. Hypoxic modulation of exogenous nitrite-induced vasodilation in humans. *Circulation* 117: 670–7, 2008.

39. **McDonagh STJ**, **Wylie LJ**, **Winyard PG**, **Vanhatalo A**, **Jones AM**. The Effects of

Chronic Nitrate Supplementation and the Use of Strong and Weak Antibacterial Agents on Plasma Nitrite Concentration and Exercise Blood Pressure. *Int J Sports Med* 36: 1177–85, 2015.

40. **McDonough P**, **Behnke BJ**, **Padilla DJ**, **Musch TI**, **Poole DC**. Control of microvascular oxygen pressures in rat muscles comprised of different fibre types. *J Physiol* 563: 903–13, 2005.

41. **Omar SA**, **Webb AJ**. Nitrite reduction and cardiovascular protection. *J Mol Cell Cardiol* 73: 57–69, 2014.

42. **Ormerod JOM**, **Arif S**, **Mukadam M**, **Evans JDW**, **Beadle R**, **Fernandez BO**, **Bonser RS**, **Feelisch M**, **Madhani M**, **Frenneaux MP**. Short-term intravenous sodium nitrite infusion improves cardiac and pulmonary hemodynamics in heart failure patients. *Circ Heart Fail* 8: 565–71, 2015.

43. **Poole DC**, **Behnke BJ**, **McDonough P**, **McAllister RM**, **Wilson DF**. Measurement of muscle microvascular oxygen pressures: compartmentalization of phosphorescent probe. *Microcirculation* 11: 317–26, 2004.

44. **Poole DC**, **Hirai DM**, **Copp SW**, **Musch TI**. Muscle oxygen transport and utilization in heart failure: implications for exercise (in)tolerance. *AJP Hear Circ Physiol* 302: H1050–H1063, 2011.

45. **Rumsey WL**, **Vanderkooi JM**, **Wilson DF**. Imaging of phosphorescence: a novel method for measuring oxygen distribution in perfused tissue. *Science (80-)* 241: 1649–1652, 1988.

46. **Schrage WG**, **Joyner MJ**, **Dinenno FA**. Local inhibition of nitric oxide and prostaglandins independently reduces forearm exercise hyperaemia in humans. *J Physiol* 557: 599–611, 2004.

47. **Shiva S**, **Sack MN**, **Greer JJ**, **Duranski M**, **Ringwood LA**, **Burwell L**, **Wang X**, **MacArthur PH**, **Shoja A**, **Raghavachari N**, **Calvert JW**, **Brookes PS**, **Lefer DJ**, **Gladwin MT**. Nitrite augments tolerance to ischemia/reperfusion injury via the modulation of mitochondrial electron transfer. *J Exp Med* 204: 2089–102, 2007.

48. **Tripatara P**, **Patel NSA**, **Webb A**, **Rathod K**, **Lecomte FMJ**, **Mazzon E**, **Cuzzocrea S**, **Yaqoob MM**, **Ahluwalia A**, **Thiemermann C**. Nitrite-derived nitric oxide protects the rat kidney against ischemia/reperfusion injury in vivo: role for xanthine oxidoreductase. *J Am Soc Nephrol* 18: 570–80, 2007.

49. **Webb A**, **Bond R**, **McLean P**, **Uppal R**, **Benjamin N**, **Ahluwalia A**. Reduction of nitrite to nitric oxide during ischemia protects against myocardial ischemia-reperfusion damage. *Proc Natl Acad Sci U S A* 101: 13683–8, 2004.

50. **Wilson DF**, **Erecinska M**, **Drown C**, **Silver IA**. Effect of oxygen tension on cellular energetics. *Am J Physiol Cell Physiol* 233: C135–140, 1977.

51. **Wilson JR**, **Hoyt RW**, **Ferraro N**, **Janicki JS**, **Weber KT**. Effect of hydralazine on nutritive flow to working canine gracilis skeletal muscle. *J Am Coll Cardiol* 4: 529–534, 1984.

52. **Wilson JR**, **Martin JL**, **Ferraro N**, **Weber KT**. Effect of hydralazine on perfusion and metabolism in the leg during upright bicycle exercise in patients with heart failure. *Circulation* 68: 425–432, 1983.

53. **Wylie LJ**, **Kelly J**, **Bailey SJ**, **Blackwell JR**, **Skiba PF**, **Winyard PG**, **Jeukendrup AE**, **Vanhatalo A**, **Jones AM**. Beetroot juice and exercise: pharmacodynamic and dose-response relationships. *J Appl Physiol* 115: 325–36, 2013.

54. **Zamani P**, **Rawat D**, **Shiva-Kumar P**, **Geraci S**, **Bhuva R**, **Konda P**, **Doulias P-T**, **Ischiropoulos H**, **Townsend RR**, **Margulies KB**, **Cappola TP**, **Poole DC**, **Chirinos JA**. Effect of inorganic nitrate on exercise capacity in heart failure with preserved ejection fraction. *Circulation* 131: 371–80; discussion 380, 2015.